IOPscience iopscience.iop.org

Home Search Collections Journals About Contact us My IOPscience

# Crystal structure and stability of β-$Na_2ThF_6$ at non-ambient conditions

This article has been downloaded from IOPscience. Please scroll down to see the full text article.

2007 J. Phys.: Condens. Matter 19 266219

(http://iopscience.iop.org/0953-8984/19/26/266219)

View the table of contents for this issue, or go to the journal homepage for more

Download details:
IP Address: 129.252.86.83
The article was downloaded on 28/05/2010 at 19:37

Please note that terms and conditions apply.

IOP PUBLISHING JOURNAL OF PHYSICS: CONDENSED MATTER

J. Phys.: Condens. Matter **19** (2007) 266219 (11pp) doi:10.1088/0953-8984/19/26/266219

# Crystal structure and stability of $\beta$-$Na_2ThF_6$ at non-ambient conditions

**Andrzej Grzechnik[1,5], Michael Fechtelkord[2], Wolfgang Morgenroth[3,4], Jose María Posse[1] and Karen Friese[1]**

[1] Departamento de Física de la Materia Condensada, Universidad del País Vasco, Bilbao, Spain
[2] Institut für Geologie, Mineralogie und Geophysik der Ruhr-Universität Bochum, Germany
[3] Institut für Anorganische Chemie, Georg-August-Universität, Göttingen, Germany
[4] Department of Chemistry, Aarhus University, Denmark

E-mail: andrzej@wm.lc.ehu.es

Received 3 May 2007, in final form 28 May 2007
Published 15 June 2007
Online at stacks.iop.org/JPhysCM/19/266219

**Abstract**

The crystal structure and stability of $\beta$-$Na_2ThF_6$ at non-ambient conditions have been studied with calorimetric analysis, second harmonic generation measurements, and $^{19}F$ and $^{23}Na$ magic-angle spinning nuclear magnetic resonance (MAS NMR) spectroscopy, as well as synchrotron x-ray single-crystal and powder diffraction. The twinned structure ($P321$, $Z = 1$) is built of chains of capped trigonal prisms around the Th atoms formed along the $c$-axis through sharing of the basal faces. More distorted capped trigonal prisms around the Na atoms share their basal and equatorial faces with each other. The twin operation is a two-fold rotation around the $c$-axis. $\beta$-$Na_2ThF_6$ is stable in the temperature and pressure ranges of 100–954 K and 0.0001–6.4 GPa, respectively. The Na–F distances are more compressible than the Th–F distances. A hypothetical *ferroelastoelectric* and *ferrobielastic* $P321 \leftrightarrow P\bar{6}2m$ phase transition is discussed.

## 1. Introduction

Crystallographic studies of complex fluorides containing the 5f elements started during the Manhattan project [1–4]. At this time, the crystal structures of these compounds were deduced from x-ray powder diffraction. The chemical composition of various phases was also determined through a detailed examination of the x-ray data. As Zachariasen put it in his own words, 'this unorthodox method of analysis had to be used because the chemical analysts were busy with more important work' [1]. Over 60 years have passed since the Manhattan Project, but the interest in complex fluorides of actinides continues due to their nuclear applications as core coolants with solid fuels, liquid fuel in a molten salt reactor, or solvents for spent nuclear solid fuel [5–7]. The modern key chemical systems contain fluorides

[5] Author to whom any correspondence should be addressed.

with thorium and alkali metals. Their structures and physical properties can now be studied with a range of sophisticated computational and experimental techniques [7–10] not available to Zachariasen [1–4].

Several polymorphs of $Na_2ThF_6$ have been reported [1–4]. In the $\alpha$ phase, isostructural with $CaF_2$ ($Fm\bar{3}m$, $Z = 4$), the Na and Th atoms are randomly distributed over the metal sites of the fluorite structure [3]. The structure of the $\beta$ phase has been described both in space group $P321$ ($Z = 1$, phase $\beta_2$) and in space group $P\bar{6}2m$ ($Z = 1$, phase $\beta_1$) [1, 2]. In both phases, the ordered Na and Th atoms have nine nearest-neighbour fluorine atoms at the corners of capped trigonal prisms. The difference between them arises from local symmetries and distortions of the Na sites, which are $C_3$ and $D_{3h}$ in space groups $P321$ and $P\bar{6}2m$, respectively. Based on the unit-cell dimensions, it might be deduced that $\delta$-$Na_2ThF_6$ (see table XII in [1]) is isostructural with $\delta$-$Na_2UF_6$ ($P3$, $Z = 2$) [11]. In this structure, two U and two Na atoms are nine-fold coordinated, while the other two Na atoms in the asymmetric unit are in the six-fold antiprismatic coordination. Relationships among all the different structural types have been discussed in [12].

It has been suggested that the $\beta$ form of disodium thorium fluoride is a *higher-order ferroic* [13–15], in which the *ferroic* and *prototypic* space groups are $P321$ and $P\bar{6}2m$, respectively [15]. The $P321 \leftrightarrow P\bar{6}2m$ phase transition is supposed to be simultaneously *ferroelastoelectric* and *ferrobielastic*. A *ferroic* crystal in general contains two or more possible orientation states (twin domains) with nearly identical physical properties [13–15]. In the absence of external forces all possible states are equal in energy. Under a certain driving force, the twin domain walls will move, switching the crystal from one orientation state to another. The twin domains in a *ferroelastoelectric* crystal differ in their piezoelectric tensors. Under applied stress, the twins strain differently in a *ferrobielastic* crystal, so one of them will be favoured over the other(s).

In this study, we have aimed at redetermining the crystal structure of $\beta$-$Na_2ThF_6$ reported by Zachariasen [1, 2] and investigating its behaviour at non-ambient conditions. The main goal has been to check whether the *higher-order ferroic* $P321 \leftrightarrow P\bar{6}2m$ phase transition is plausible in the $\beta$ form of disodium thorium fluoride. Our experimental techniques have included calorimetric analysis, second harmonic generation measurements, and $^{19}F$ and $^{23}Na$ magic-angle spinning nuclear magnetic resonance (MAS NMR) spectroscopy, as well as synchrotron x-ray single-crystal and powder diffraction.

## 2. Experimental methods

A single crystal of $\beta$-$Na_2ThF_6$ was grown with the Czochralski method; it came from the same batch as the one investigated with Raman and infrared spectroscopies by Teixeira *et al* [16]. A part of it was finely ground for thermal analysis, NMR spectroscopy, and x-ray diffraction measurements.

Differential scanning calorimetry was performed using the systems Pyris 1 and 7 (Perkin-Elmer) in the temperature range from 290 to 954 K.

Qualitative second harmonic generation measurements were carried out on an unoriented single crystal using a Q-switched $Nd^{3+}$:YAG laser ($\lambda = 1064$ nm, pulse width 6 ns, pulse frequency 5 Hz).

NMR spectra were recorded on a Bruker ASX 400 NMR spectrometer. The $^{19}F$ MAS NMR spectra were obtained at 376.43 MHz using a standard Bruker 4 mm MAS probe. Typical conditions were pulse lengths of 4.0 $\mu$s (the 90° pulse length for liquid $p$-$C_6H_4F_2$ was 8.0 $\mu$s) and 30 s recycle delays for $^{19}F$. Thirty two scans were accumulated at a MAS rotation frequency of 4, 8, 12.5 and 15 kHz for the $^{19}F$ MAS NMR spectra. A liquid $p$-$C_6H_4F_2$ sample ($\delta = -120.0$ ppm with respect to liquid $CFCl_3$) was used for the $^{19}F$ spectra as reference

standard. The $^{23}$Na MAS NMR experiments were performed at 105.85 MHz in a 4 mm high rotation standard MAS probe. Typical conditions were pulse lengths of 0.6 $\mu$s for the $^{23}$Na NMR experiments and recycle delays of 500 ms. A total of 22 000 scans for the $^{23}$Na NMR experiments were accumulated at a MAS rotation frequency of 12.5 kHz. The $^{19}$F NMR spectra as well as the $^{23}$Na MAS NMR spectra were fitted with chemical shift anisotropy lineshapes and quadrupolar lineshapes using the DMFIT2005 program [17].

X-ray diffraction experiments at room temperature and ambient pressure were performed at ANKA Synchrotron Light Source in Karlsruhe (Germany). The powder pattern was collected at the *Diff* Beamline (in Bragg–Brentano geometry, $\lambda = 0.953\,45$ Å, with a $2\theta$ range of 6°–66°, and an angular step of 0.004°). Single-crystal intensities were measured using a Stoe IPDS II diffractometer at the *Single-Crystal Diffraction* Beamline ($\lambda = 0.7999$ Å).

Single-crystal and powder x-ray measurements at high pressures and room temperature as well as single-crystal x-ray measurements at 100 K and atmospheric conditions were carried out using a HUBER four-circle diffractometer (equipped with a marCCD165 detector) at the *D*3 Beamline in HASYLAB (Hamburg, Germany). A finely ground sample was loaded into a DXR-6 (Diacell) diamond anvil cell for powder experiments with monochromatic radiation at 0.4 Å. The collimator slits were set to 50 $\mu$m × 50 $\mu$m. The images were integrated with the program FIT2D to yield intensity versus $2\theta$ diagrams [18]. The ruby luminescence method [19] was used for pressure calibration and a 1:4 mixture of ethanol:methanol was used as a hydrostatic pressure medium. A fluorite powder was added as an internal standard for the $2\theta$ calibration at each pressure through the $CaF_2$ equation of state [20]. A series of x-ray intensity measurements was carried out at high pressure on a single crystal (approximately $40 \times 10 \times 30$ $\mu$m$^3$) with a synchrotron beam collimated to 0.4 mm. The diamond cell was of the Ahsbahs type (the opening angle of 90°) [21]. The diamond culets (600 $\mu$m) were modified by laser machining so that the angle between them and the tapered parts of the diamonds was 40°. A 250 $\mu$m hole was drilled into a stainless steel gasket preindented to a thickness of 80 $\mu$m. The intensities at all pressures were collected upon compression. The ruby luminescence method [19] was implemented for pressure calibration and a 1:4 mixture of ethanol:methanol was used as a hydrostatic pressure medium. Due to the particular semi-spherical cut of the diamonds, no absorption correction was necessary for the diamond anvils. The intensities were integrated and corrected with the program XDS [22]. The reflections from $Na_2ThF_6$ overlapping with the reflections from the diamonds could easily be identified because of their very large intensities, and they were rejected. The reflections from the crystal in the shaded areas of the detector were excluded using the criterion $I < 6\sigma(I)$. A small number of reflections overlapping with the Debye–Scherrer rings of the gasket material were also excluded. The single-crystal intensities at 100 K were measured using an Oxford Instruments cryojet ($\lambda = 0.55$ Å). They were integrated and corrected with the program XDS [22].

## 3. Results and discussion

The results of thermal analysis indicate that $\beta$-$Na_2ThF_6$ does not undergo any phase transition in the temperature range 290–954 K. Its crystal structure is confirmed to be non-centrosymmetric since the second harmonic generation effect was qualitatively detected.

The $^{19}$F MAS NMR spectra show two different signals with an isotropic chemical shift of $\delta_{iso} = -31.2$ ppm and $-0.5$ ppm for two different crystallographic fluorine sites in the structure of $\beta$-$Na_2ThF_6$ (figure 1 and table 1). Both sites show equal signal intensities, i.e., the same crystallographic multiplicity. Site 2 seems to possess a higher coordination number than site 1 because of the lower isotropic chemical shift. The deviation from spherical (cubic) coordination is higher for site 2, while the deviation from axial symmetry is much higher for

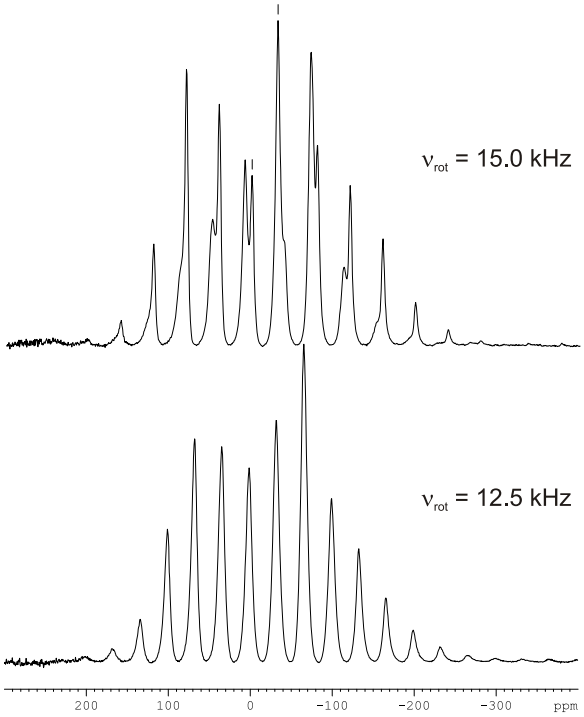


**Figure 1.** $^{19}$F MAS NMR spectra of $\beta$-$Na_2ThF_6$ at two different rotational frequencies. The marked signals are the isotropic chemical shifts of the two fluorine sites.

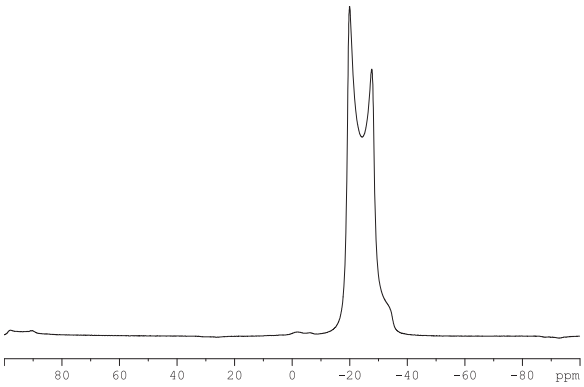


**Figure 2.** $^{23}$Na MAS NMR spectrum of $\beta$-$Na_2ThF_6$.

site 1. The $^{23}$Na MAS NMR spectrum (figure 2) contains one resonance, a quadrupolar pattern with the quadrupolar coupling constant $C_Q = 1.79$ MHz and the asymmetry parameter $\eta = 0.0$, meaning that the Na atom is at an axial symmetric site. Such a local structure of $\beta$-$Na_2ThF_6$ in principle agrees with both structural models for the $\beta_1$ (space group $P\bar{6}2m$) and $\beta_2$ (space group $P321$) phases [1, 2].

The x-ray powder diagram measured at room temperature and ambient pressure (*Diff* Beamline, ANKA Synchrotron Light Source, Karlsruhe) could be indexed with a hexagonal unit cell: $a_0 = 5.983\,02(9)$ Å, $c_0 = 3.834\,01(9)$ Å, and $V_0 = 118.857(4)$ Å$^3$, respectively.

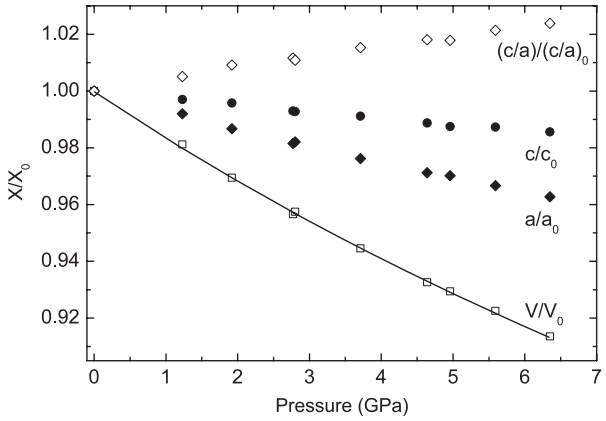


**Figure 3.** Pressure dependence of the normalized lattice parameters, unit-cell volume, and $c/a$ axial ratio; $a_0 = 5.983\,02(9)$ Å, $c_0 = 3.834\,01(9)$ Å, and $V_0 = 118.857(4)$ Å$^3$. The line is the Murnaghan equation-of-state fit to the compressibility data: $V_0 = 118.9(1)$ Å$^3$, $B_0 = 58(1)$ GPa, $B' = 4.00$.

**Table 1.** Parameters extracted from the $^{19}$F MAS NMR spectra for the fluorine atoms in $Na_2ThF_6$. $\delta_{iso}$ is an isotropic chemical shift, FWHH is a halfwidth of the signal, $\delta_{CSA}$ is a chemical shift anisotropy and $\eta$ is an asymmetry parameter.

| Site | $\delta_{iso}$ (ppm) | FWHH (ppm) | $\delta_{CSA}$ (ppm) | $\eta$ | Rel. intensity (%) |
|---|---|---|---|---|---|
| 1 | −31.2 | 8.1 | 108.4 | 0.7 | 50 |
| 2 | 0.5 | 5.5 | −204.7 | 0.4 | 50 |

The x-ray powder patterns collected at high pressures provide evidence that $\beta$-$Na_2ThF_6$ is structurally stable at least to 6.4 GPa, with no indication of a change of symmetry. The compressibility data shown in figure 3 were extracted using the program Chekcell for the unit-cell refinement [23]. They could be fitted with the Murnaghan equation of state to give the zero-pressure bulk modulus $B_0$ and the unit-cell volume at ambient pressure $V_0$ (for the fixed first pressure derivative of the bulk modulus $B' = 4.00$) equal to 58(1) GPa and 118.9(1) Å$^3$, respectively. This material is more compressible along the $a$-axis, so the $c/a$ axial ratio increases at high pressures.

The key problem to resolve from an analysis of the single-crystal data was the determination of the correct symmetry. The two non-centrosymmetric space groups suggested in the earlier investigations [1, 2] are in a group–subgroup relationship: the space group $P321$ is a maximal subgroup (an index $t = 2$) of the hexagonal space group $P\bar{6}2m$. Accordingly, the corresponding structures are expected to be very similar. We therefore tried different models in the structure refinement [24] process (table 2) using the data set collected at 100 K and ambient pressure.

The first model (model 1) was in space group $P\bar{6}2m$ with Na in the Wyckoff position 2d (2/3, 1/3, 1/2), Th in 1a (0,0,0), F1 in 3f ($x$, 0, 0), and F2 in 3g ($x$, 0, 1/2). Although the overall agreement factors were satisfactory, a detailed inspection of the difference and $F_{obs}$ Fourier maps showed a considerable residual electron density close to the Th position. This difference could be accounted for by introducing a tensor of fourth order to refine the displacement parameters for this atom (model 2). Such an anharmonic refinement lowered

**Table 2.** Details of different refinements for a single crystal of $Na_2ThF_6$ at 100 K and ambient pressure (HASYLAB, $\lambda = 0.55$ Å). No. pars and No. refl. are the number of parameters and the number of observed reflections.

| Model | Space group | $wR_{obs}$ | $GoF_{obs}$ | No. pars | No. refl. | $u_{33}$ (Na) | Remarks |
|---|---|---|---|---|---|---|---|
| 1 | $P\bar{6}2m$ | 0.0367 | 2.52 | 14 | 1531 | 0.082(5) | Th harmonic |
| 2 | $P\bar{6}2m$ | 0.0236 | 1.62 | 18 | 1531 | 0.082(3) | Th anharmonic |
| 3 | $P\bar{6}2m$ | 0.0234 | 1.61 | 19 | 1531 | 0.033(3) | Na-split atom |
| 4 | $P321$ | 0.0235 | 1.53 | 22 | 2196 | 0.083(2) | |
| 5 | $P321$ | 0.0226 | 1.47 | 23 | 2196 | 0.034(2) | Twin model |

the overall agreement factor.[6] While the Th and F atoms seemed to be well described in the anharmonic refinement (model 2), the same was not true for the Na atom, which showed a strong elongation of its anisotropic displacement parameter in the $z$-direction, $u_{33} = 0.082(3)$. Considering the fact that the low-temperature data set was used for the refinements and that this parameter was approximately 10 times larger than the corresponding parameters $u_{11}$ and $u_{22}$, this value of 0.082(3) was not reasonable. We attributed this feature to a structural disorder of the Na atoms. Hence, we placed the Na atom at the general position 4h $(2/3, 1/3, z)$ in model 3. This split-atom model with the Na–Na distance of 0.381(6) Å did not lower the final agreement factors significantly, but had a substantial influence over the anisotropic displacement parameters as $u_{33}$ decreased to 0.033(3).

This observation suggested lowering the symmetry to space group $P321$ and placing the Na atom in the Wyckoff position 2d $(2/3, 1/3, z)$, Th in 1a (0, 0, 0), F1 in 3e $(x, 0, 0)$ and F2 in 3f $(x, 0, 1/2)$ (model 4). Final agreement factors were comparable to the earlier ones. However, the $z$-coordinate of Na refined to a value that was essentially equal to $1/2$. i.e., the refined model was equivalent to model 2 but with too low a symmetry. Again, the Na atom showed a very large elongation of the displacement ellipsoid in the direction of the $c$-axis. Assuming a twin model (model 5) in this space group with an additional two-fold rotation around the $c$-axis as a twin operation, i.e. with the symmetry element vanishing in the symmetry reduction $P\bar{6}2m \rightarrow P321$, the Na atom moved to a position $z = 0.548(1)$, while at the same time the parameter $u_{33}$ reduced significantly. The final agreement factors were better than those for all the other refinements. Therefore, our preferred structural model for $\beta$-$Na_2ThF_6$ studied here is model 5 in space group $P321$ (table 3)[7].

The anharmonic character of the displacement parameters of the Th atoms might be a sign of a possible symmetry reduction at even lower temperatures than 100 K. A new hypothetical polymorph might be the $\delta$ phase [1], supposedly isostructural with $\delta$-$Na_2UF_6$ (space group $P3$) [11]. In this structure, the $c$-parameter is doubled with respect to the one for $\beta$-$Na_2ThF_6$. The position of the Th atom would thus be split into two positions, both being on the three-fold axis with their $z$-coordinates no longer symmetry related. Consequently, a tendency of $\beta$-$Na_2ThF_6$ (space group $P321$) to transform to space group $P3$ should lead to an elongation of the displacement parameters of Th in the direction of the $c$-axis. What we observe, however, is an elongation of the Th displacement parameters in the $(x, y)$-plane, suggesting that the Th atom rather tends to move away from its ideal position on the three-fold axis. It is possible to reach comparable overall agreement factors to the ones for model 5, assuming a further symmetry reduction to monoclinic space group $P2$. However, this happens at the cost of a

[6] The anharmonic displacement parameters were also used in models 3–5.

[7] The isotropic Gaussian extinction coefficient $G_{iso}$ was also refined. Further details of the crystallographic investigations (tables 3 and 4) can be obtained from the Fachinformationszentrum Karlsruhe, D-76344 Eggenstein-Leopoldshafen, Germany, on quoting the depository numbers CSD 418141–418148.

**Table 3.** Experimental and structural data for the single-crystal measurement at 100 K and ambient pressure (HASYLAB, $\lambda = 0.55$ Å).

| Crystal data | |
|---|---|
| $a$ (Å) | 5.9390(6) |
| $c$ (Å) | 3.8130(3) |
| $V$ (Å$^3$) | 116.47 |
| $\rho$ (g cm$^{-3}$) | 5.587 |
| $\mu$ (mm$^{-1}$) | 33.316 |
| $G_{\rm iso}$ | 0.010(1) |
| **Data collection** | |
| No. measured refl. | 2283 |
| Range of $hkl$ | $-9 \leqslant h \leqslant 16$ |
| | $0 \leqslant k \leqslant 19$ |
| | $0 \leqslant l \leqslant 11$ |
| No. observed refl.[a] | 2196 |
| $R(\rm int)_{obs}$[b] | 1.66 |
| $\sin(\theta)/\lambda$ | 1.6021 |
| **Refinement**[b] | |
| $R_{\rm obs}$ | 1.98 |
| $wR_{\rm obs}$ | 2.26 |
| $GoF_{\rm obs}$ | 1.47 |
| No. parameters | 23 |
| **Structural parameters** | |
| Twin volume I (%) | 45.2(4) |
| Twin volume II (%) | 54.8(4) |
| $z$ (Na) | 0.548 (1) |
| $U_{\rm iso}$ (Na) | 0.016 9(8) |
| $U_{\rm iso}$ (Th) | 0.003 88(8) |
| $x$ (F1) | 0.619 0(3) |
| $U_{\rm iso}$ (F1) | 0.011 3(4) |
| $x$ (F2) | 0.251 6(2) |
| $U_{\rm iso}$ (F2) | 0.007 6(2) |

[a] The criterion for observed reflections is $|F_{\rm obs}| > 3\sigma$.
[b] All agreement factors are given in %; weighting scheme $1/[\sigma^2(F_{\rm obs}) + (0.01F_{\rm obs})^2]$.

larger number of parameters in the refinement compared to the one for the anharmonic model in $P321$ (43 parameters versus 23 parameters).

The refinements of the high-pressure and room-temperature ambient-pressure (table 4) data were consequently performed using model 5 (see footnote 7). Since these data were measured to relatively low $\sin\theta/\lambda$-values, all the atoms (including Th) were refined with harmonic displacement parameters[8]. For the sake of consistency of all these refinements, the $u_{33}$ parameters of the Na atoms for the measurements at 1.15–4.89 GPa and at ambient pressure were fixed at the value of 0.03(1) refined from the data set collected at 0.22 GPa.

[8] Models 1 and 3–5 listed in table 2 could essentially be refined with harmonic displacement parameters using any single-crystal data measured for this study. Model 5 is superior in every case. The high $f''$ values for the Th atom at $\lambda = 0.4$, 0.55, and 0.7999 Å allow for an unambiguous determination of one of the two possible enantiomorphic orientations.

**Table 4.** Experimental and structural data for the single-crystal measurements at room temperature and high pressures.

| Pressure (GPa) | 0.0001 | 0.22 | 1.15 | 1.18 | 2.27 | 3.55 | 4.89 |
|---|---|---|---|---|---|---|---|
| | | | Crystal data | | | | |
| $a$ (Å) | 5.985(2) | 5.976(1) | 5.9371(5) | 5.9361(5) | 5.8936(8) | 5.8490(5) | 5.8054(6) |
| $c$ (Å) | 3.843(1) | 3.830(1) | 3.8212(6) | 3.8205(4) | 3.8109(6) | 3.7991(4) | 3.7878(6) |
| $V$ (Å$^3$) | 119.21 | 118.45 | 116.65 | 116.59 | 114.64 | 112.56 | 110.56 |
| $\rho$ (g cm$^{-3}$) | 5.458 | 5.4494 | 5.579 | 5.582 | 5.676 | 5.781 | 5.886 |
| $\mu$ (mm$^{-1}$) | 32.546 | 32.759 | 33.266 | 33.283 | 33.850 | 34.475 | 35.099 |
| $G_{iso}$ | 0.8(2) | 0.15(1) | 0.12(1) | 0.12(2) | 0.14(1) | 0.11(1) | 0.10(1) |
| | | | Data collection | | | | |
| Facility | ANKA | HASYLAB | HASYLAB | HASYLAB | HASYLAB | HASYLAB | HASYLAB |
| λ (Å) | 0.7999 | 0.4 | 0.4 | 0.4 | 0.4 | 0.4 | 0.4 |
| No. measured refl. | 550 | 2472 | 2354 | 2382 | 1509 | 2354 | 1689 |
| Range of $hkl$ | $-7\leqslant h\leqslant 7$ | $-10\leqslant h\leqslant 10$ | $-10\leqslant h\leqslant 10$ | $-10\leqslant h\leqslant 10$ | $-10\leqslant h\leqslant 10$ | $-10\leqslant h\leqslant 10$ | $-10\leqslant h\leqslant 10$ |
| | $-7\leqslant k\leqslant 7$ | $-11\leqslant k\leqslant 10$ | $-10\leqslant k\leqslant 10$ | $-9\leqslant k\leqslant 10$ | $-10\leqslant k\leqslant 10$ | $-10\leqslant k\leqslant 10$ | $-9\leqslant k\leqslant 10$ |
| | $-5\leqslant l\leqslant 5$ | $-6\leqslant l\leqslant 6$ | $-6\leqslant l\leqslant 6$ | $-6\leqslant l\leqslant 6$ | $-6\leqslant l\leqslant 6$ | $-6\leqslant l\leqslant 6$ | $-6\leqslant l\leqslant 6$ |
| No. observed refl.[a] | 161 | 494 | 459 | 454 | 444 | 446 | 427 |
| $R(\text{int})_{obs}$[b] | 11.76 | 8.51 | 8.68 | 9.00 | 6.53 | 7.17 | 6.80 |
| $\sin(\theta)/\lambda$ | 0.6592 | 0.9399 | 0.9235 | 0.9352 | 0.9199 | 0.9230 | 0.9179 |
| | | | Refinement[b] | | | | |
| $R_{obs}$ | 4.50 | 3.11 | 3.17 | 3.79 | 3.02 | 3.07 | 3.17 |
| $wR_{obs}$ | 6.52 | 3.44 | 3.43 | 4.62 | 3.56 | 3.66 | 3.37 |
| $GoF_{obs}$ | 6.82 | 2.20 | 2.22 | 3.17 | 2.23 | 2.52 | 2.12 |
| No. parameters | 17 | 18 | 17 | 17 | 17 | 17 | 17 |
| | | | Structural parameters | | | | |
| Twin volume I (%) | 43.6(4.5) | 52.0(1.6) | 50.0(1.7) | 55.6(2.2) | 50.6(1.8) | 50.5(1.9) | 50.3(1.8) |
| Twin volume II (%) | 56.4(4.5) | 48.0(1.6) | 50.0(1.7) | 44.4(2.2) | 49.4(1.8) | 49.5(1.9) | 49.7(1.8) |
| $z$ (Na) | 0.558(6) | 0.554(3) | 0.551(2) | 0.552(3) | 0.548(2) | 0.547(3) | 0.543(3) |
| $U_{iso}$ (Na) | 0.025(3) | 0.023(3) | 0.023(1) | 0.022(1) | 0.021(1) | 0.021(1) | 0.022(1) |
| $U_{iso}$ (Th) | 0.024(2) | 0.0055(1) | 0.0056(1) | 0.0060(1) | 0.0061(1) | 0.0057(1) | 0.0059(1) |
| $x$ (F1) | 0.618(6) | 0.620(1) | 0.618(2) | 0.616(2) | 0.614(1) | 0.614(2) | 0.609(1) |
| $U_{iso}$ (F1) | 0.04(1) | 0.026(3) | 0.024(4) | 0.023(4) | 0.023(3) | 0.019(3) | 0.021(3) |
| $x$ (F2) | 0.251(3) | 0.253(1) | 0.251(1) | 0.252(1) | 0.253(1) | 0.254(1) | 0.254(1) |
| $U_{iso}$ (F2) | 0.012(5) | 0.020(2) | 0.019(3) | 0.020(3) | 0.018(3) | 0.015(2) | 0.018(2) |

[a] The criterion for observed reflections is $|F_{obs}| > 3\sigma$.
[b] All agreement factors are given in %; weighting scheme $1/[\sigma^2(F_{obs}) + (0.01F_{obs})^2]$.

The results of our structural refinements show that the relative twin volumes are not sensitive to changes in the unit-cell volume (tables 3 and 4). On the other hand, the $z$-coordinate of the Na atom exhibits a tendency to converge to the value of 1/2 upon compression (table 4 and figure 4).

Figure 5 shows the crystal structure of $\beta$-$Na_2ThF_6$ ($P321$, $Z = 1$) in different projections. Chains of capped trigonal prisms around the Th atoms are formed along the $c$-axis through sharing of the basal faces. The more distorted prisms around the Na atoms share their basal and equatorial faces with each other. The F1 atom is coordinated to four Na atoms (two distances of about 2.53 Å and two distances of about 2.83 Å) and one Th atom that together form a distorted square pyramid. The F2 atoms is tetrahedrally coordinated to two Na atoms and two Th atoms.

The Na–F distances are more compressible than the Th–F distances (figure 6). Upon compression, the polyhedra around the Na atoms become more regular as the two Na–F1 distances to the basal fluorine F1 atoms (figure 5) tend to converge. Unlike the square pyramid around the F1 atom, the tetrahedron around the F2 atom becomes more distorted at elevated pressure.

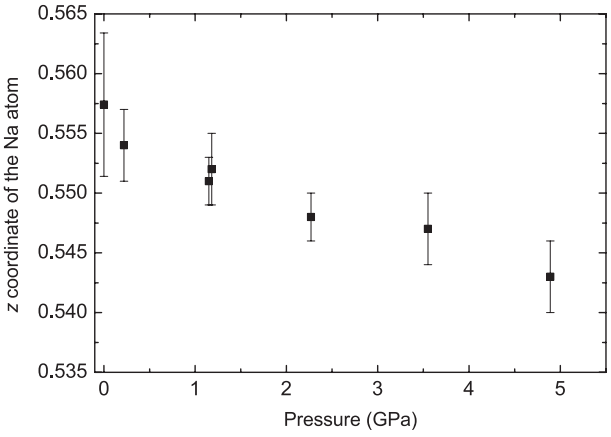


**Figure 4.** Pressure dependence of the $z$-coordinate of the Na atom.

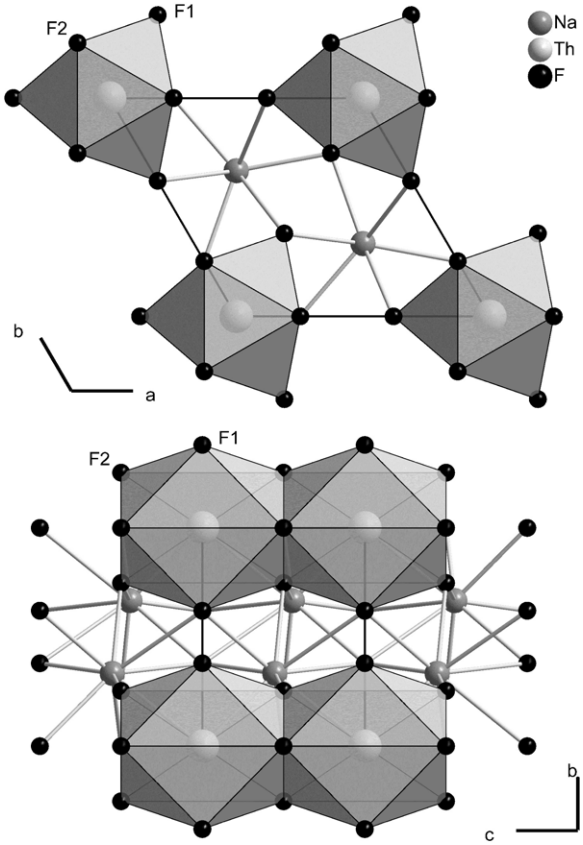


**Figure 5.** Crystal structure of $Na_2ThF_6$ at 0.22 GPa (see table 4). The F1 and F2 atoms are labelled. The polyhedra around the Th atoms are drawn.

## 4. Conclusions

The results of our work on the crystal structure of $\beta$-$Na_2ThF_6$ using modern experimental methods have in principle confirmed what Zachariasen already found out during the Manhattan Project [1, 2]. Some differences are apparent when a few details are considered. The structure is twinned in space group $P321$ with the twin operation being an additional two-fold rotation

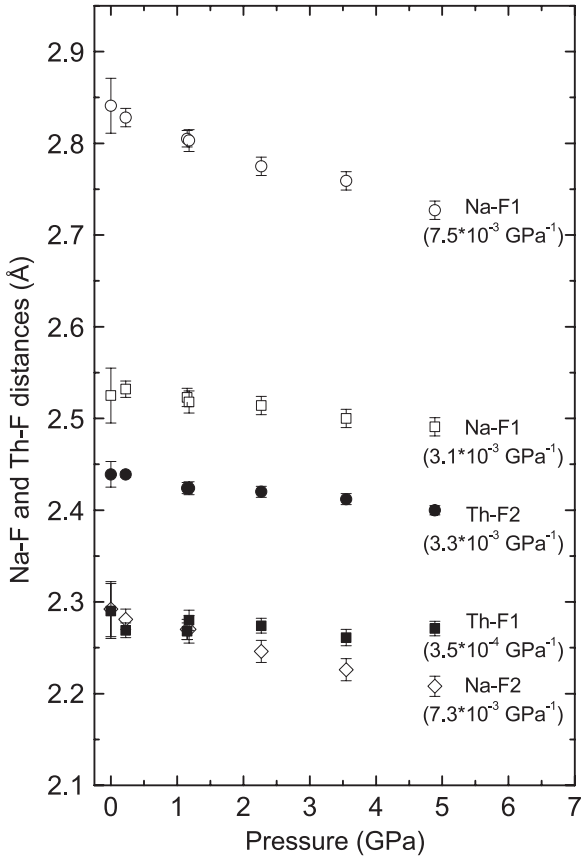


**Figure 6.** Pressure dependence of the Na–F and Th–F distances. The numbers in brackets are the bond compressibilities $\beta_{ij} = (-1/R_{ij})(\mathrm{d}R_{ij}/\mathrm{d}P)$ in the $\mathrm{GPa}^{-1}$ units.

around the $c$-axis. It is one of the symmetry elements that vanish in the symmetry reduction $P\bar{6}2m \rightarrow P321$.

In this study, we have determined that no structural transformation occurs in twinned $\beta$-$Na_2ThF_6$ ($P321$, $Z = 1$) when only temperature or pressure are changed in the ranges 100–954 K or 0.0001–6.4 GPa, respectively. The only indirect evidence for $\beta$-$Na_2ThF_6$ to be a *ferroic* could be the existence of the twin domains. The $P321 \leftrightarrow P\bar{6}2m$ phase transition would convert the twinning operation used for the description of the trigonal structure in model 5 (table 2) into a true symmetry element of the hexagonal space group $P\bar{6}2m$. To recover this symmetry, the $z$-coordinate of the Na atom would have to assume the ideal value of $1/2$. Indeed, the pressure-induced tendency of the $z$-coordinate of the Na atom to converge to this value (table 4 and figure 4) indicates that the $P321 \leftrightarrow P\bar{6}2m$ transformation could be facilitated at high pressures. Whether the *ferroelastoelectric* and *ferrobielastic* [13, 15] phase transitions indeed occur in $\beta$-$Na_2ThF_6$ warrants further studies under more suitable external fields.

## Acknowledgments

The single crystal of $\beta$-$Na_2ThF_6$ was grown by J-Y Gesland (Univ. Le Mans, France). We thank E Bocanegra and C Folcia (both at Univ. País Vasco, Spain) for the calorimetric and

second harmonic generation measurements, respectively. S Doyle and G Buth helped us with our powder and single-crystal x-ray diffraction measurements at ANKA, respectively. AG and KF acknowledge financial support from the Ministerio de Ciencia y Tecnología and the Gobierno Vasco.

## References

[1] Zachariasen W H 1948 *J. Am. Chem. Soc.* **70** 2147
[2] Zachariasen W H 1948 *Acta Crystallogr.* **1** 265
[3] Zachariasen W H 1949 *Acta Crystallogr.* **2** 388
[4] Zachariasen W H 1949 *Acta Crystallogr.* **2** 390
[5] Moir R W and Teller E 2005 *Nucl. Technol.* **151** 334
[6] Le Brun Ch 2007 *J. Nucl. Mater.* **360** 1
[7] van der Meer J P M and Konings R J M 2007 *J. Nucl. Mater.* **360** 16
[8] Konings R J M and Hildebrand D L 1998 *J. Alloys Compounds* **271–273** 583
[9] Gagliardi L, Skylaris C-K, Willets A, Dyke J M and Barone V 2000 *Phys. Chem. Chem. Phys.* **2** 3111
[10] Rivas-Silva J F, Durand-Niconoff J S and Berrondo M 2000 *Comput. Mater. Sci.* **18** 193
[11] Cousson A, Tabuteau A, Pagès M and Gasperin M 1979 *Acta Crystallogr.* B **35** 1198
[12] Grzechnik A, Bouvier P, Mezouar M, Mathews M D, Tyagi A K and Köhler J 2002 *J. Solid State Chem.* **165** 159
[13] Newnham R E 1974 *Am. Mineral.* **59** 906
Newnham R E and Cross L E 1974 *Mater. Res. Bull.* **9** 927
Newnham R E and Cross L E 1974 *Mater. Res. Bull.* **9** 1021
[14] Dudnik E F, Kushnerev A I and Duda V M 1999 *Mater. Res. Innov.* **2** 309
Akimov S V, Dudnik E F, Duda V M and Tomchakov A N 2004 *Ferroelectrics* **307** 13
Akimov S V, Duda V M, Dudnik E F, Kushnerev A I and Tomchakov A N 2006 *Phys. Solid State* **48** 1073
[15] Tolédano P and Tolédano J-C 1977 *Phys. Rev.* B **16** 386
[16] Teixeira E, Mendes Filho J, Melo F E A, Ayala A P, Gesland J-Y, Paschoal C W A and Moreira R L 2003 *Vib. Spectrosc.* **31** 159
[17] Massiot D, Fayon F, Capron M, King I, Le Calvé S, Alonso B, Durand J O, Bujoli B, Gan Z and Hoatson G 2002 *Magn. Reson. Chem.* **40** 70
[18] Hammersley A P, Svensson S O, Hanfland M, Fitch A N and Häusermann D 1996 *High Pressure Res.* **14** 235
[19] Piermarini G J, Block S, Barnett J D and Forman R A 1975 *J. Appl. Phys.* **46** 2774
Mao H K, Xu J and Bell P M 1986 *J. Geophys. Res.* **91** 4673
[20] Angel R J 1993 *J. Phys.: Condens. Matter* **5** L141
[21] Ahsbahs H 1995 *Z. Kristallogr.* **9** (Suppl.) (42)
Ahsbahs H 2004 *Z. Kristallogr.* **219** 305
[22] Kabsch W 1993 *J. Appl. Crystallogr.* **26** 795
[23] Laugier J and Bochu B http://www.inpg.fr/lmgp
[24] Petricek V, Dusek M and Palatinus L 2000 *Jana2000 The Crystallographic Computing System* (Praha: Institute of Physics)